Springer

Journal of
Mechanical
Science and
Technology

Journal of Mechanical Science and Technology 22 (2008) 134~140

www.springerlink.com/content/1738-494x

Laser induced transition from soot generation to shell shaped carbon nanoparticles in an acetylene flow: aerosol characterization

Young Jeong Kim, Sanghoon Lee, Peter Pikhitsa and Mansoo Choi*

National CRI Center for Nanoparticle Control, Advanced Institute of Machinery and Design, School of Mechanical and Aerospace Engineering, Seoul National University, Seoul, 151-742, Korea

(Manuscript Received December 8, 2006; Revised November 10, 2007; Accepted November 12, 2007)

Abstract

Shell shaped carbon nanoparticles were synthesized from acetylene flow injected inside an oxygen-hydrogen diffusion flame when it was irradiated with a focused beam of a CW CO_2 laser above a certain laser power and at a certain position [1]. In the present study, the evolution of carbon nanoparticles generated under laser irradiation has been investigated together with a study on the visualization of particle generating flames. The size distributions of carbon shell nanoparticles and soots have been determined by examining the images of TEM grid on which particles were captured by local thermophoretic sampling. The variations of radii of gyration and fractal dimensions of soot and shell shaped particulate aggregates are obtained at different laser powers.

Keywords: Nanoparticle; Flame synthesis;Laser irradiation

1. Introduction

Since carbon nanomaterials such as carbon nanotubes [2], carbon onions [3] and fullerene-related nanoforms were synthesized, carbon nanomaterials have become a center of interest for nanotechnology. Many researchers think of the unique properties of carbon nanotubes having concentric shells of graphene layers in a cylindrical form that may be utilized for future applications such as Li ion batteries [4], gas storage media, cold electron field emitters [5], etc. Carbon nanomaterials such as fullerenes and carbon nanotubes are also considered to be promising materials as electrochemical mediators and enzyme stabilizers [6].

Because of the existence of bent graphene layers in these carbon nanomaterials, they have their own unique properties. As it has been shown in our recent papers [7, 8], it would be this alternation of metallic and semiconducting regions within curved layers of nanocarbons that provides a low voltage threshold and high emission current for cold electron field emission from nanostructured carbon materials. Therefore, there is a strong need to find an industrially attractive pathway to synthesize nanocarbons having varying curvatures and, moreover, to investigate their properties in many aspects such as electrical and mechanical ones. Previously, we developed a method synthesizing shell shaped carbon nanoparticles (SCNPs) having curved graphene layers in a spherical form at large scale [1, 9]. In the method, an assistant oxy-hydrogen diffusion flame was utilized for preheating acetylene which undergoes CW CO_2 laser irradiation. We showed that laser irradiated acetylene flow could generate well crystallized shell shaped carbon nanoparticles above a certain laser power and at a certain position. In the present study, we carry out a study on the detailed evolution of carbon nanoparticles generated under laser irradiation together with a study of visualization of particle generating flames. The variations of radii of gyration and fractal dimensions of carbon nanoparticles are reported at different laser powers.

*Corresponding author. Tel.: +82 2 880 7128, Fax.: +82 2 878 2465
E-mail address: mchoi@snu.ac.kr
DOI 10.1007/s12206-007-1016-7

2. Experimental

Fig. 1 shows our experimental setup. The multi annular nozzles in our co-flow burner were fed with C_2H_2 as a central gas flow, N_2 as an inner shield gas, H_2 and O_2, as an outer oxy-hydrogen diffusion flame cone, and air for outer stabilization, respectively. It is noted that in the present study, C_2H_2 is not the fuel for flame but the chemical precursor for carbon nanoparticles. All flow rates of gases were controlled with mass flow controllers (MKS, 1179A). The flow rates are 1 lpm for hydrogen, 0.5 lpm for oxygen, 0.35 lpm for nitrogen as an inner shield, and 0.1 lpm for acetylene. Acetylene, injected into H_2-O_2 flame, was then irradiated with a CW CO_2 laser (Bystronic, BTL 2800). Power levels were changed up to 2500W in this experiment and beam diameter at the flame was adjusted to be 3mm by ZnSe lens (focal length 150mm). Laser irradiation in a particle generating flame was previously utilized to control the size, morphology, and crystalline phase of silica [10] and titania nanoparticles [11, 12]. One can control the laser irradiating position onto the flame with a traversing system. For sampling particles out of the flame on the TEM grid, we used an *in situ* local sampling device which takes advantage of the thermophoretic force [13, 14]. The dwelling time of a TEM grid in flame can be set as desired in the range of 1 ms by using sets of timers. The local thermophoretic sampling device consists of a sampling probe holding a TEM grid, a shield covering the TEM grid, two air cylinders and three timers to control the insertion times of the probe and the shield independently. The shield covers the probe to prevent deposition of particles on the grid when the probe is inserted into the desired local point in a flame and pulled out of the flame. The shield has been designed to retract and expose the grid during the sampling duration only after the probe is located at the desired local position within the flame. The grids were examined with TEM (Transmission Electron Microscope) for measuring the primary particle size distribution, the radius of gyration and the fractal dimension of aggregates.

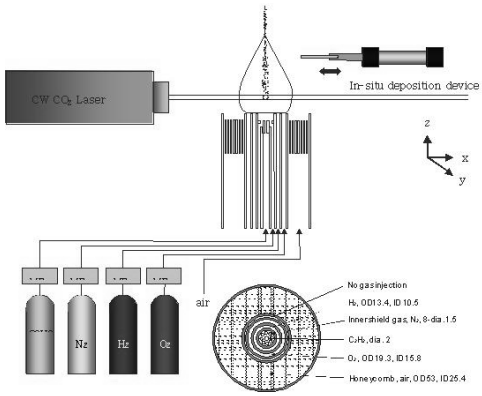

Fig. 1. Experimental setup for laser induced transition from soot generation to shell shaped carbon nanoparticles.

To locate and visualize the reaction before and after the irradiation onto the flame, ICCD camera (Roper Scientific, PI-PIAX 512 RB) was used. To collect the light signal from the reaction zone, other light sources were blocked. It was done because when the transition occurs the luminosity of the reaction is too intensive; the shutter time of ICCD camera was adjusted as well. No filter was used. This light signal is delivered to the ICCD camera and then is taken as an image in a personal computer for analysis.

The crystallinity of particles was investigated with X-ray diffractometer. The X-ray diffractometer (M18XHF-SRA, MAC Science Co.) measures diffraction signal from 10 degree to 90 degree with a step of 4 degrees per minute.

3. Results and Discussion

First, we examined the generation of carbon soot particles from acetylene gas heated in an oxy-hydrogen flame without laser irradiation and their growth with respect to flame heights. The results are shown in Fig 2. In the conventional flame without laser irradiation, primary seeds of soot particles were found from the location higher than 11mm for the given conditions. Those seeds are initially shown as non-agglomerates at 11 mm and 13 mm, but, as soot particles grow with flame, these become aggregates consisting of many primary particles. When laser beam is irradiated at 15mm flame height where carbon soots exist(see Fig. 3(a)), it was found that the originally premature soots shown in Fig. 3(b) were changed into mature soots of the fully aggregate shape at different laser powers (see Fig. 3(c)-(e)). Even though laser irradiation was shown to change the size and morphology of carbon soot, it was not possible to change the crystalline phase of carbon particles when the laser irradiated the existing soot particles. All the cases when the laser irradiated the existing soot only resulted in usual carbon soot in which discontinuous BSU(Basic Structural Units)

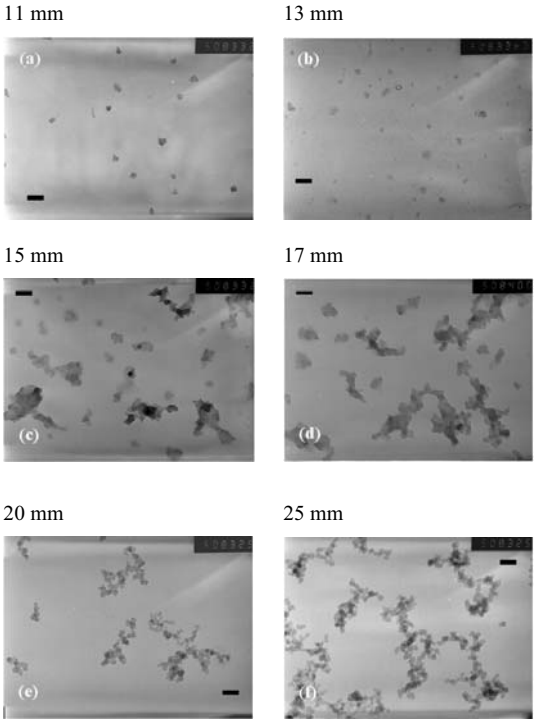

Fig. 2 Evolution of soot particles generated from acetylene in an oxyhydrogen flame (scale bar 100 nm)

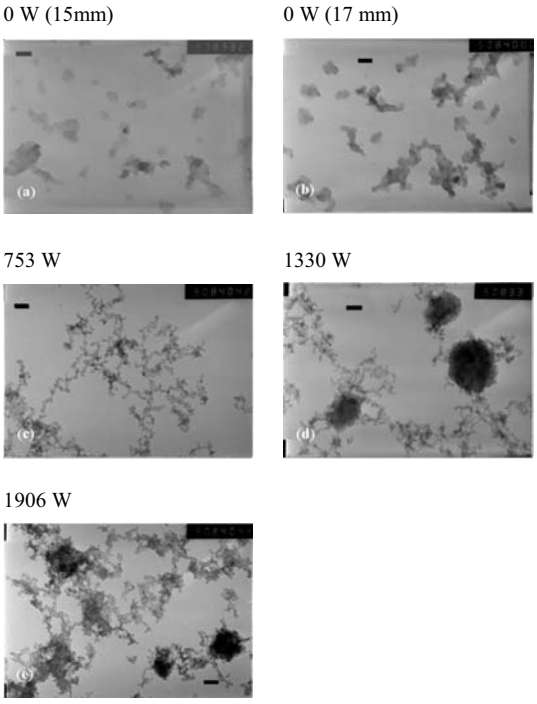

Fig. 3. Changes in size and morphology of carbon soot particles with laser irradiation on soots in a flame (h_i : 15 mm, h_s : 17 mm, scale bar 100nm).

[15] existed randomly.

With 10mm incidence of the laser where carbon soot does not exist, shell-shaped carbon particles were generated at a laser power of 1880W as shown in Fig. 4(f) and nearly all particles were SCNPs. With low laser powers, we produced aggregates of soot particles as shown in Fig. 4(a)-(e) though there might be possibility that some minor portion of shell particles could exist but were not detected by TEM images. The SCNPs are of high crystallinity consisting of several graphene layers and are hollow in the center. As evidenced by the cases with laser irradiation on existing soots, SCNPS are not the result of transformation of existing soots. A surprising fact is that our laser induced transition occurs without any sensitizers added in the flame. Furthermore, C_2H_2 and other gases injected are non-absorbing 10.6 μm laser beam. It is speculated that preheating of acetylene by the outer oxyhydrogen flame could generate laser beam absorbing intermediates such as ethylene which may absorb the laser beam and generate carbon vapor to be eventually condensed to form shell shaped carbon nanoparticles. It is again emphasized that SCNPs are

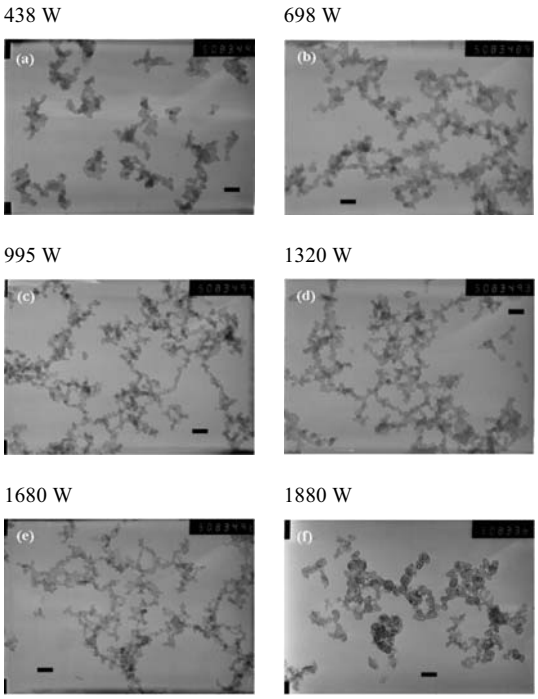

Fig. 4. Variation of carbon nanoparticles with laser irradiation where carbon soot particles do not exist. The case of 1880 W shows that almost all particles are shell shaped carbon nanoparticles (SCNPs) (h_i : 10 mm, h_s : 15 mm, Scale bar 100 nm).

not created in the way of restructuring of mature soot particles. To produce SCNPs, the laser irradiating height in the flame should be fixed on the point where soot is not found, which is the major difference between samples shown in Fig. 3 and Fig. 4. Even with the same laser power, we cannot produce SCNPs when flame is irradiated at the point where mature soot is found (in this case, above 11 mm).

We reported a high resolution TEM image of shell-shaped particles shown in Fig. 4(f) [1]. From the image (Fig. 5(b)), the high crystallinity of SCNPs is clearly seen in comparison to the structure of soot in Fig. 5(a). The soot has an irregular arrangement of disconnected BSU. On contrary, from Fig. 5(b) we can distinguish the continuous and curved graphene layers in the particle. An interesting phenomenon of sudden change in flame appearance, accompanied with the transition to the production of SCNPs has been reported [1]. We can tell whether SCNPs are created or not by observing the change of luminosity of the flame. Once the condition is established to uniformly produce SCNPs (for example, the case of 2100 W in Fig. 6(a)), the luminosity of the flame increases dramatically, while the change in the luminosity of a sooting flame is small with the same laser power (the case of 2100 W in Fig. 6(b)). In the case of irradiation on 10 mm, the length of flame is getting slightly shorter as the laser power goes up before it reaches the 'transition' point. Once it reaches the transition power, the luminosity of flame goes high enough to make one unable to see it with the naked eye with a bright tail of particles above the reaction point (Fig. 6(a)). We visualized the particle producing aspect in the flame with ICCD camera which enables one to detect the point where particles are generated as well as the relative variation of intensity level of luminosity of the reactions. A normal flame without laser irradiation shows the low level of luminosity (~ 2400 in arbitrary unit) (see Fig. 7(a)). With a laser power of 1400W, there is not a big difference in flame shape only to show small increase of luminosity (Fig. 7(b)). Once the full transition happens, the reaction is confined within the vicinity of the point where laser is irradiated with a two order of magnitude increase of luminosity level (Fig. 7(c)). The left flame image of Fig. 7(c) clearly shows the particle stream survived from oxidation while ICCD image cannot show the particle stream due to the big difference in luminosity level between the particle stream and the reaction point. This big difference of

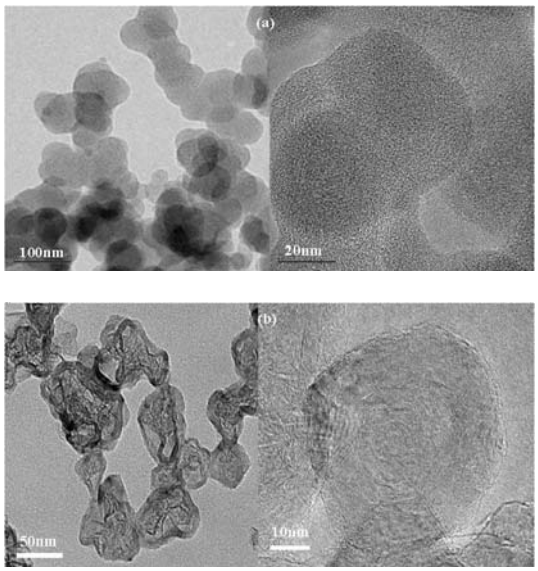

Fig. 5. TEM/HRTEM images of carbon nanoparticles (a) soot (b) shell shaped carbon nanoparticle (adapted from [1]).

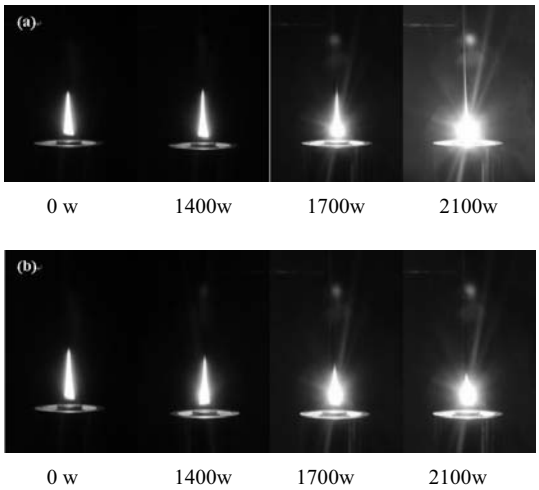

Fig. 6. Flame pictures with irradiation onto (a) 10mm above the burner, (b) 15mm above the burner (All pictures were taken with shutter speed of 1/5sec and lens aperture of F6.3).

the luminosity level is an indication of full generation of shell-shaped carbon nanoparticles. Even though the luminosity level in the particle stream is small compared to that in the reaction zone, the intensity is much higher than the flame without laser irradiation (the case of Fig. 7(a)).

The difference between soot and SCNPs is not only in the structure but also in the size distribution of primary particles. From TEM image analysis, the primary particle size distribution of SCNPs was

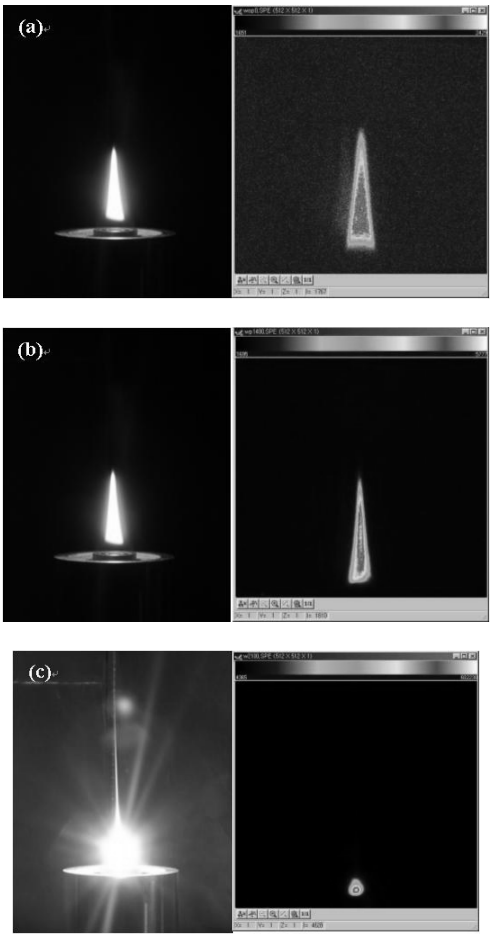

Fig. 7. Flame pictures and ICCD camera images in the case of laser powers (a) 0 W, (b) 1400 W, (c) 2100 W.

measured (Fig. 8). For this measurement, we had to measure more than 2000 particles per each case to ensure statistically reliable data. The diameter used in Fig.8 is the Martin's diameter which we adopted for measurement due to random orientation of particles. In this distribution, three cases represent the soot particle distribution corresponding to the laser powers of 1400 W, 1500 W, and 1600 W. When the laser power is not fully sufficient to produce all particles being SCNPs as in the case of 1700 W, a bimodal distribution can be observed due to the co-existence of soots and SCNPs, where the soot can be regarded as a contamination of the new SCNP phase. The 2100 W case is characterized by a unimodal SCNP distribution, which indicates full generation of SCNPS and the primary particle sizes of shell-shaped carbon nanoparticles are much larger than those of soot particles.

The mean radius of gyration and fractal dimension

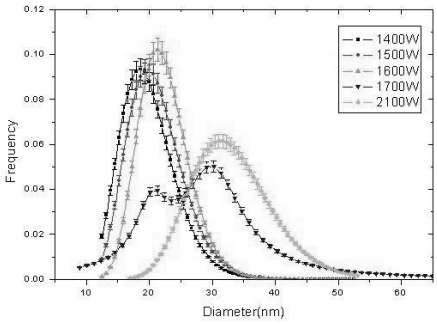

Fig. 8. Primary particle size distributions of carbon nanoparticles generated with different laser powers.

of nanoparticle aggregates are shown in Fig. 9. The mean radius of gyration gets bigger as we increase the laser power up to 800 W (Fig. 9(a)). And it becomes smaller as the power of the laser increases further. On the other hand, the fractal dimension decreases slightly with a laser power increase up to 1000 W and then increases again to around 1.9 as the laser power increases to 2100 W (Fig. 9(b)). The evolution of the mean radius of gyration and fractal dimension with the laser power can be understood by taking into account the processes in acetylene conversion into solid carbon. Indeed, let the acetylene soot aggregates at zero laser power be characterized by some initial mean primary particle size, cluster radius of gyration, and fractal dimension. It is known [16] that primary soot particles are charged and their colliding (and subsequent "gluing" together with the help of surface reactions of acetylene decomposition) is greatly influenced by the charging in ionization processes in flame. Indeed, soot particles tend to be aggregated in nearly one-dimensional chains. Those chains produce the secondary cluster-cluster aggregates (distinguished by the ring-like structures in Fig. 3 and 4) on the later stage of the soot formation. The longer the chains, the lower the fractal dimension of the resulting cluster may be.

As it is seen from TEM images (Fig. 3), with the increase in the laser power the lengths of chains seen in an individual cluster become larger. It may be an indication of enhanced ionization and charging processes in the laser-induced plasma. (This plasma is a pre-requisite for the following direct laser-induced conversion of acetylene into carbon vapor and continuous layers of SCNPs.). Naturally, if the one- dimensional chains grow longer, the overall fractal dimension of the cluster of chains may decrease (due to prevalenceof one-dimensional chains in the struc-

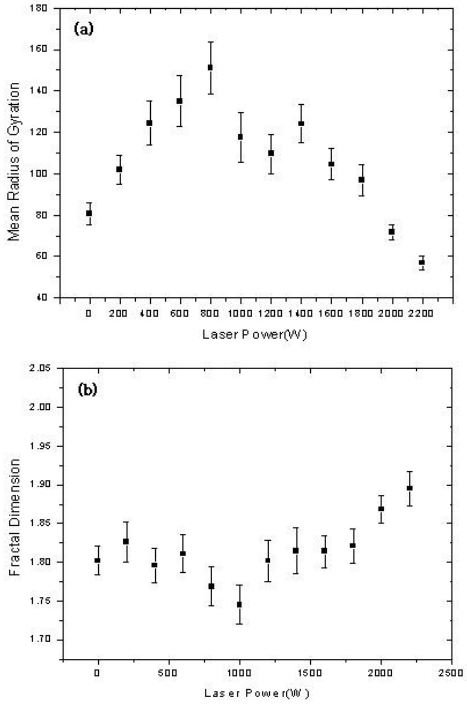

Fig. 9. Mean radius of gyration and fractal dimension of aggregates of carbon nanoparticles for different laser powers (a) mean radius of gyration, (b) fractal dimension.

ture), yet its radius of gyration increases. It is exactly what is observed in experiment (see Fig. 9).

When the laser power increases more, a small amount of SCNPs can start to be generated at some laser power near 1000 W. It is noted that within the laser beam diameter (~ 3 mm), there should be variations in the velocity and concentration of C_2H_2, which may cause the transition to the partial production of shell particles to occur at a certain location within the beam diameter. This partial SCNP generation competes with the soot generation in a way that "gluing" surface reactions which survived from soot generation become more and more unfavorable. The "chains" of the SCNPs become shorter and there is a general tendency at a very high laser power to have individual primary particles instead of chain-like aggregates. In parallel, radius of gyration starts going down though the fractal dimension grows up. It should be noted that this change in the radius of gyration and in fractal dimension does not happen necessarily at one and the same laser power because the process of "gluing" pure SCNPs together (with the help of the surface reaction) proceeds even at high laser power and thus delays the compacting and the increase in fractal dimension (compare Fig. 9(a) and Fig. 9(b), where the maximum in radius of gyration and minimum in fractal dimension are at slightly different laser power).

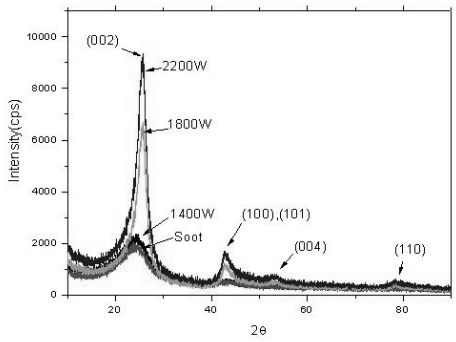

Fig. 10. X-ray diffraction pattern of carbon nanoparticles for different laser powers.

Fig. 10 shows the x-ray diffraction pattern of SCNPs. There are several well-defined crystal planes which make SCNPs distinguishable from soot. Those planes are (002), (100), (101), (004), and (110) for SCNPs. From the intensities of the peak located at around 25 degrees of four samples indicated, we are able to compare the degree of crystallization for each sample. The samples with the transition (1800W and 2200W cases) exhibit narrow and big intensity peaks at 25 degrees whereas the samples without the transition (1400W, soot cases) show broad and low intensity peaks. Although the two different phases – SCNPs and soot particles – are easily distinguished one from the other in TEM images, the X-ray diffraction pattern (XRD) given in Fig. 10 demonstrates somewhat smoothed evolution with increasing laser power from broad soot peaks towards sharp XRD peaks of pure SCNPs of high graphitization. This can be understood as a consequence of the gradual evolution of the bimodal distribution of the two phases reflected in their primary particle size distribution given in Fig. 8.

4. Conclusions

SCNPs were synthesized by using the irradiation of a CW CO_2 laser onto the oxygen-hydrogen diffusion flame with C_2H_2 as a precursor. We found that the observed formation of SCNPs was not a restructuring of mature soot formed in flame. This was proved by considering the case of the irradiation of CO_2 laser on the sooting region in flame in which case no SCNPs were found. The sooting flame and SCNP producing

reaction were taken by a digital camera and ICCD camera as well, which enables one to estimate the aspect of the reaction zone. Especially with those images we could observe that SCNPs can survive oxidation and exit the reaction zone. The size distribution of primary SCNPs showed that they were larger than soot primary particles. The structural characteristics from XRD demonstrated that SCNPs had a good crystallinity when compared to soot. The results of the measurement of radius of gyration and fractal dimension of soot and SCNPs indicate different producing processes for soot particles and for SCNPs that have to be learned in future research.

Acknowledgments

This work was funded by the Creative Research Initiative program supported by the Ministry of Science and Technology, Korea.

References

[1] M. Choi, I.S. Altman, Y. J. Kim, P. V. Pikhitsa, S. H. Lee, G. Park, T. Jeong and J. Yoo, Formation of shell-shaped carbon nanoparticles through critical transition in irradiated acetylene, *Advanced Materials* 16 (19) (2004) 1721-1725.

[2] S. Iijima, Helical microtubules of graphitic carbon, *Nature* 354 (1991) 56.

[3] D. Ugarte, Curling and closure of graphitic networks under electron-beam irradiation, *Nature* 359 (1992) 707.

[4] G. Maurin, C. Bousquet, F. Henn, P. Bernier, R. Almairac and B. Simon, Electrochemical intercalation of lithium into multiwall carbon nanotubes, *Chemical Physics Letters* 312 (1) (1999) 14-18.

[5] J. M. Bonard, M. Croci, C. Klinke, R. Kurt, O. Noury, and N. Weiss, Carbon nanotube films as electron field emitters, *Carbon* 40 (10) (2002) 1715-1728.

[6] S. B. Yoon, K. Sohn, J. -Y. Kim, C. -H. Shin, J. -S. Yu and T. Hyeon, Fabrication of carbon capsules with hollow macroporous core/mesoporous shell structures, *Advanced Materials*, 14 (1) (2002) 19-21.

[7] I. S. Altman, P. V. Pikhitsa and M. Choi, Two-process model of electron field emission from nanocarbons: temperature effect, *Journal of Applied Physics* 96 (6) (2004) 3491-3493.

[8] I. S. Altman, P. V. Pikhitsa and M. Choi, Electron field emission from nanocarbons: a two-process model, *Applied Physics Letters* 84 (2004) 1126-1128.

[9] M. Choi, S. H. Lee, J. Y. Hwang, Method for manufacturing shell shaped fine carbon particles, Korean patent, no. 0385574 (2003).

[10] D. Lee and M. Choi, Control of size and morphology of nano particles using CO_2 laser during flame synthesis, *Journal of Aerosol Science* 31 (2000) 1145-1163.

[11] D. Lee and M. Choi, Coalescence enhanced synthesis of nanoparticles to control size, morphology and crystalline phase at high concentrations, *Journal of Aerosol Science* 33 (2002) 1-16.

[12] D. Lee, S. Yang and M. Choi, Controlled formation of nanoparticles utilizing laser irradiation in a flame and their characteristics, *Applied Physics Letters* 79 (2001) 2459-2461.

[13] J. Cho and M. Choi, Determination of number density, size and morphology of aggregates in coflow diffusion flames using light scattering and local sampling, *Journal of Aerosol Science* 31 (9) (2000) 1077-1095.

[14] R. A. Dobbins and C. M. Megaridis, Morphology of flame-generated soot as determined by thermophoretic sampling, *Langmuir* 3 (2) (1987) 254-259.

[15] A. Galvez, N. Herlin-Boime, C. Reynaud, C. Clinard and J-N. Rozaud, Carbon nanoparticles from laser pyrolysis, *Carbon* 40 (2002) 2775-2789.

[16] A. A. Onischuk, S. di Stasio, V. V. Karasev, A. M. Baklanov, G. A. Makhov, A. L. Vlasenko, A. R. Sadykova, A. V. Shipovalov and V. N. Panfilov, Evolution of structure and charge of soot aggregates during and after formation in a propane/air diffusion flame, *Journal of Aerosol Science* 34 (2003) 383-403.